Ligand-dependent changes in the SPR of magnetic nanoparticles

L. Radu[*], D. Caruntu[*], M. White[*], J. Wiley[*], C.J. O'Connor[*], P. Hanson[*†]

[*]Department of Chemistry, University of New Orleans,
New Orleans, LA, USA, 70148
phanson@uno.edu

ABSTRACT

Magnetite nanoparticles of 12.7 nm in diameter were studied by superparamagnetic resonance (SPR) at X-band frequency (9.4 GHz). Two methods were used that yielded particles with very different SPR spectra. The particles were studied with ligands, such as salts and proteins, immobilized onto the particle surface. The characteristic lines and line-shapes of Fe^{2+} and Fe^{3+} highlight the sensitivity of SPR to changes in the coordination sphere of the particles. For example, the presence of the g~4 resonances reveals distortions to the packing of the F^{3+} ions within the nanoparticles. The SPR spectra of magnetite appear to be acutely sensitive to alteration of the chemical environment. Lineshape parameters relating to the anisotropy and crystal structure (ΔB_{eff}, g_{eff}, A) detail ligand-dependent changes within the SPR spectra.

Keywords: superparamagnetic resonance, magnetic nanoparticles,

1 INTRODUCTION

The magnetic properties of iron oxide nanoparticles make them candidates for applications such as magnetic contrast agents[1], novel surface coatings[2], and drug delivery vehicles[3]. While the structural features of magnetic nanoparticles are typically characterized by methods such as scanning electron microscopy, the magnetic behavior of iron-oxide particles is usually characterized using methods as SQUID. Enhanced detail of the magnetic characteristics of iron-oxide nanoparticles comes from super-paramagnetic resonance (SPR) studies. SPR is distinguished from electron paramagnetic resonance (EPR) in that SPR investigates systems containing many unpaired electrons while EPR typically involves systems of isolated electrons. SPR provides information about a magnetic particle's size distribution and shape[4, 5], its magnetic anisotropy[6], concentration, and the coordination environment of the ions.

SPR studies of ferrite nanoparticles have shown that nanoparticle size-distribution, particle shape, chemical environment, temperature and particle concentration determine the line-shape of the SPR spectrum[4]. Recent efforts using proteins with defined cages for nucleating and growing nanoparticles have successfully developed iron-oxide ferrite nanoparticles of specific sizes[7]. SPR data acquired at multiple frequencies, from S-band to D-band, suggest that variations from bulk magnetization values are surface-dependent in particles with diameters below 20 nm. In this work, the SPR characterization of 13 nm magnetite nanoparticles is used to elucidate the link between the chemical-material attributes and the performance of *de novo* biomagnetic nanoparticles.

2 EXPERIMENTAL

2.1 Superparamagnetic Resonance (SPR)

SPR experiments were performed with a Bruker EMX spectrometer equipped with a TE_{102} cavity, goniometer, and variable temperature option. Samples of magnetite were transferred to a 100 μL quartz capillary, then flame-sealed. Data were acquired with 2-6 mW of power, a spectral width of 8000 Gauss at centerfield of 4000 Gauss. The modulation amplitude used for the experiments was 10 Gauss, significantly less than the narrowest linewidth. The time constant was 41 ms, the conversion time was 81.6 ms, and frequency modulation was 100 kHz for each experiment. In cases where the nanoparticles settled out of solution, the solution was vortexed immediately prior to transfer into a quartz capillary, then flame sealed.

The first-derivative of the power absorption was monitored as a function of the applied field (H_1) with the maxima and minima in the derivative signal defining the peak-to-peak distance. At the zero-crossing point in the first-derivative spectrum, the derivative of the power is zero (dW/dB=0) and defines the effective resonance field (g_{eff}). The temperature dependence of the samples was studied from 100-370 K with increments of 10 K and accuracy of +/- 0.1 K.

2.2 Magnetite Nanoparticle Synthesis and SPR Sample Preparation

Two types of magnetite nanoparticles were provided with diameters of 12.7 nm. Their synthesis resulted from the hydrolysis of chelated alkoxide complexes of Fe^{2+} and Fe^{3+} in solutions of diethylene glycol (DEG) and N-methyl diethanol amine (NMDEA) or DEG and diethanol amine (DEA) at high temperature[8]. The resulting magnetite nanoparticles were stored in methanol after extensive washing to remove the chelating agents. For the studies in this paper, the nanoparticles were either studied in methanol or methanol solutions with salts. Transfer of the particles into the methanol salt solutions was accomplished by first

isolating the particles with a permanent magnet, washing 3x with the desired solution, then re-suspending the particles in 100 μL of solution and subsequently transferred into a quartz capillary, that was then flame-sealed for SPR analysis.

3 RESULTS

Based upon transmission electron microscopy (TEM), the magnetite nanoparticles in this study have a diameter of 12.7 and **blah** nm +/- 1 nm. High-resolution TEM revealed the particles to be single-domain structures. The distribution of Fe^{2+} and Fe^{3+} ions is such that Fe^{3+} ions occupy octahedral and tetrahedral sites within the lattice (figure 1) while Fe^{2+} ions occupy octahedral sites. Octahedral↔tetrahedral Fe^{3+} anti-ferromagnetic coupling (yellow arrow) effectively limits the magnetic behavior of the particles to Fe^{3+}↔ Fe^{2+} ferromagnetic coupling (black arrow) across the octahedral sites (figure 1A) within the nanoparticles.

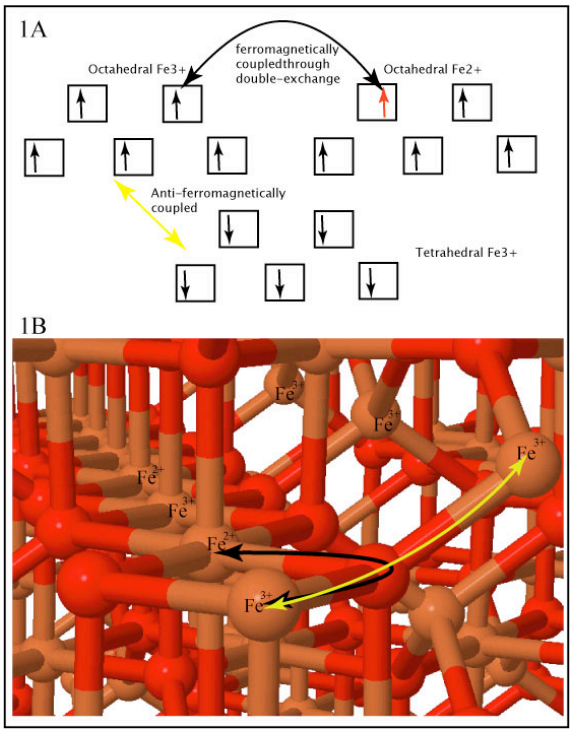

Figure 1. (A) The magnetic behavior of magnetite nanoparticles is dependent upon a double exchange mechanism that effectively limits the SPR signal to octahedral Fe^{3+}↔Fe^{2+} ferromagnetic coupling (black arrow). (B) Model view of inverse-spinel magnetite showing the octahedral and tetrahedral sites.

The stock solution of ~20 mg/mL magnetite showed evidence of inter-particle dipolar exchange through increased linewidths (data not shown). Dipolar exchange effects can be minimized by obtaining data from a magnetically dilute sample. The concentration for obtaining the magnetically dilute solutions was determined from a series of dilutions and subsequent SPR acquisitions (data not shown). The lineshapes of the SPR spectra sharpened asymptotically to ~2 mg/mL magnetite nanoparticle. Below ~ 2mg/mL, the SPR line-shapes remained unchanged and the solutions were deemed magnetically dilute.

SPR data were collected across a temperature range of 170-270 K with the data from the temperature limits presented in figure 2. The presented data are scaled to approximately the same peak intensity. The SPR spectra of magnetite particles prepared from DEA/DEG (figure 2A) are dramatically different from spectra acquired with nanoparticles prepared from NMDEA/DEG (figure 2B). The doublet at g_{eff}~3.59 (figure 2A, 170 K) is characteristic of high-spin Fe^{3+} in a rhombic crystal field[9]. The presence of a doublet in this g_{eff} region is the trademark spectroscopic signature of Fe^{3+} in two states, historically labeled $Fe^{3+}_{(I)}$ and $Fe^{3+}_{(II)}$[10]. As the temperature decreases,

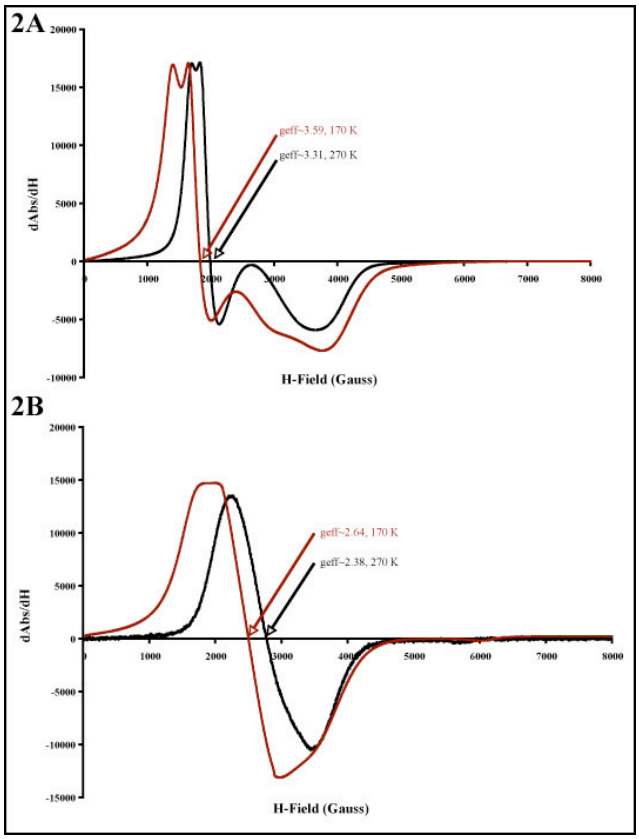

Figure 2. The SPR data from magnetite prepared from DEA/DEG (2A) and NMDEA/DEG (2B) reveal the preparations yield particles with different degrees of order.

there is a linear increase of the g_{eff}; below 170 K, the g_{eff} begins to decrease (data not shown). The resolution increases for the g_{eff}~4 doublet and the resonances near g_{eff}~2 as the temperature decreases. The broad linewidth (ΔH > 1000 Gauss) of the g_{eff}~2 transition is representative

of super-paramagnetic iron oxides. The linewidth increases linearly as the temperature of the sample is decreased to ~170 K then begins to display the same deviations from linearity observed with g_{eff}.

The magnetite samples prepared from NMDEA/DEG (figure 2B) yield broadened signals from super-paramagnetic iron oxides along with axially and rhombically distorted Fe^{3+}. As the temperature is lowered, the g_{eff} values increases until the spectrum resembles a broadened version of figure 2A.

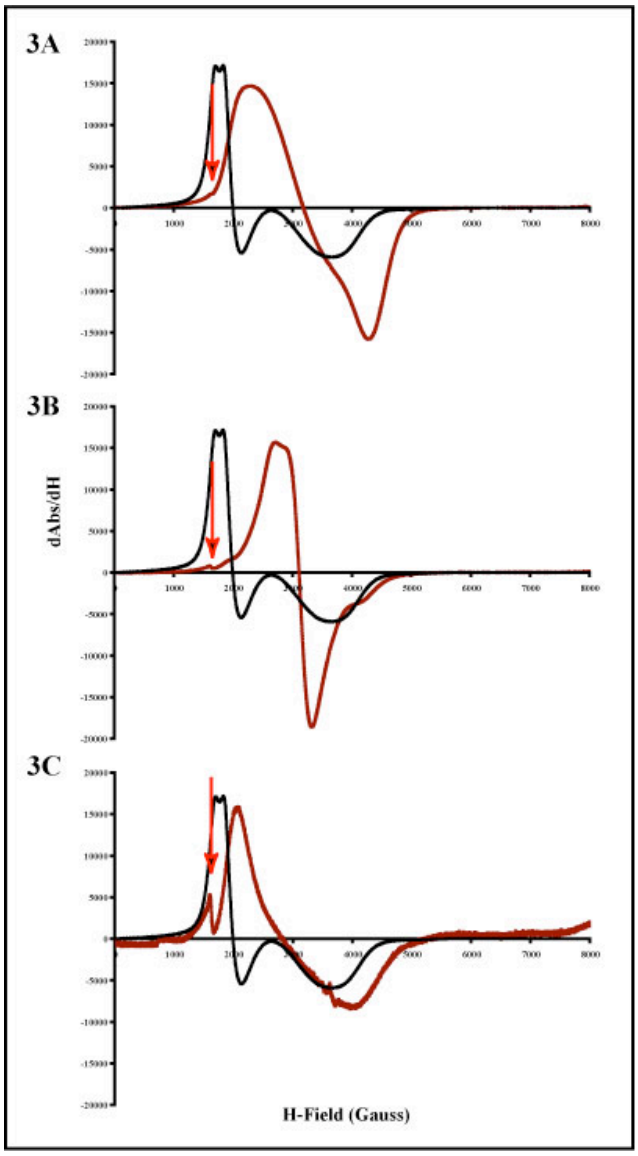

Figure 3. Magnetite from the NMDEA/DEG preparation suspended in methanol (black) with sodium carbonate (A, red), sodium acetate (B, red), and BSA (C, red).

The Fe^{2+} and Fe^{3+} ions at the surface of the nanoparticles have incomplete coordination spheres. As a result, the presence of ligands such as carbonate and acetate should complete the coordination of Fe^{2+}/Fe^{3+} ions. To test this hypothesis, the magnetite particles from figure 2A were suspended in solutions of methanol containing 0.1 M sodium carbonate (figure 3A) or sodium acetate (figure 3B). The g_{eff}~4, g_{eff}~2 transitions, and line-widths undergo significant changes in the presence of these salts. The g_{eff}~4 resonances of distorted Fe^{3+} seem to shift to higher magnetic field values and/or merge with the g_{eff}~2 super paramagnetic iron-oxide resonances; however, some residual absorbance from the g_{eff}~4 remains (red arrow). The g_{eff}~2 undergoes a dramatic sharpening in the presence of acetate(figure 3B) in contrast with the distortions with carbonate (figure 3A).

An alternative approach in the coordination of ligands to the surface is to use a protein or polypeptide. The side-chains of proteins and polypeptides include ligation groups, such as carboxylates and amino groups, that could coordinate to the Fe^{2+}/Fe^{3+} ions at the surface of magnetite. When the protein bovine serum albumin, BSA, was added to the nanoparticles (figure 3C) the resulting line-shape is intermediate between that of 3A and 3B with the exception of the larger remnant of the g_{eff}~4 transition.

4 DISCUSSION

Magnetite has an inverse-spinel structure that places Fe^{3+} in the octahedral and tetrahedral positions of the lattice while Fe^{2+} occupies the remaining octahedral position within the lattice (figure 1A). High resolution TEM images show that a modest variation in preparation of magnetite nanoparticles, substituting N-methyl-diethylamine for diethylamine, yield single-domain particles of the same size[8], but dramatically different SPR spectra (figure 2). Neither spectrum displays the canonical two-line pattern of one broad and one sharp resonance centered at g_{eff}~2[11]. The spectra also provide little in the way of similarity with other magnetite nanoparticles studied by SPR[12-14]. While the data have several spectroscopic differences, there are behaviors they have in common.

In both cases, the particles experience dipolar relaxation at concentrations in excess of 5 mg/mL. Magnetically dilute samples are achieved in solutions below 2 mg/mL. The g_{eff} and linewidths of the spectra increase linearly with decreasing temperature in both nanoparticle preparations. Single crystals of magnetite are historically known for having a g_{eff}~2 when the applied field is aligned with the particles' easy axis of magnetization[9, 15]; higher g_{eff} values result with other orientations relative to the applied field. This angular dependence results in dramatic increases in linewidth as the nanoparticles have their easy axis randomly immobilized with respect to the applied field with decreasing temperature[4]. The coincident linear changes in g_{eff} and linewidth for the two particles indicates they are single-domain[6] that is in agreement with high-resolution TEM imagery[8]; however, deviations from linearity begin to occur at 170 K. Magnetite undergoes a conversion from a high-temperature cubic phase to a low-temperature mono-clinic phase below ~125 K, the Verwey

transition (T_v). Above T_v, the charge between Fe^{2+}/Fe^{3+} hops readily between the two ions and both octahedral iron ions can be described as $Fe^{2.5+}$. Below T_v, the charges become fixed with the resulting change in ion behavior leading to distortions of the crystal structure. The cubic→monoclinic phase transition will lead to distortions of the crystal field that should manifest changes in the SPR spectra[9]. Alternatively, the nanoparticles in this study were suspended in methanol. Methanol becomes polycrystalline at lower temperature and may lead to artificial increases in the local nanoparticle concentration through occlusion of the particles from the crystalline structure. Such behavior would lead to the return of dipolar interactions and non-linear behavior of g_{eff} and linewidth.

For the particles prepared from DEA/DEG (figure 2A), superparamagnetic iron oxide (g_{eff}~2) is present along with high-spin Fe^{3+} in a rhombic crystal field (g_{eff}~4)[9, 15]. The spectra from figure 2A suggest the structure of the particles is of the inverse spinel type. Alternatively, transitions at g_{eff}~2 can be due to octahedral Fe^{3+} in the spinel structure of γ-phase[6]. The absence of a signal from high-spin Fe^{3+} (g_{eff}~4) from the particles prepared with NMDEA/DEG (figure 2B) suggests the particles have a spinel structure. These differences can be a product of subtle rearrangements during the annealing process of the particles.

Transitions at g_{eff}~4 are characteristic of high-spin Fe^{3+} in a rhombic crystal field[9] and the observation of a doublet in the g_{eff}~4 region is indicative of Fe^{3+} in two states[16]. At the surface where the coordination state of Fe^{3+}/Fe^{2+} ions goes unfulfilled, or within the structure of the particle where oxygen vacancies occur, the exchange interaction that leads to the ferromagnetic behavior can break down (figure 1A). These defects become minimized as ligands bind to the surface and re-establish the axially symmetric state of the Fe^{3+} ions. The resulting changes would reduce crystal field distortions and lead to reduction of the g_{eff}~4 transitions (figure 3). The observation of the g_{eff}~4 transition increasing with increasing ligand size is intriguing. The size of BSA, average molecular weight 67,000, prevents a solution to all the surface defects. As a result, the g_{eff}~4 transition would be expected to be largest for this surface modification.

In this work, SPR spectra of magnetite nanoparticles have revealed a wealth of information about the structure of the particles as well as providing details about surface changes to the nanoparticles.

5 AKNOWLEDGEMENTS

This work was sponsored by grants from the National Science Foundation Research Experiences for Undergraduates (DMR-0243977), DARPA Biomagnetics (HR0011-04-0068), the Petroleum Research Fund (38516-GB4), and the Louisiana Board of Regents (LBOR0050PR00C).

REFERENCES

[1] Byrne, S.J., et al., *Magnetic nanoparticle assemblies on denatured DNA show unusual magnetic relaxivity and potential applications for MRI.* Chem Commun (Camb), 2560-1, 2004

[2] Rossi, L.M., A.D. Quach, and Z. Rosenzweig, *Glucose oxidase-magnetite nanoparticle bioconjugate for glucose sensing.* Anal Bioanal Chem, 380, p. 606-13, 2004

[3] Ito, A., et al., *Magnetite nanoparticle-loaded anti-HER2 immunoliposomes for combination of antibody therapy with hyperthermia*. Cancer Lett, 212, p. 167-75, 2004

[4] Berger, R., et al., *Temperature Dependence of Superparamagnetic Resonance of Iron Oxide Nanoparticles*. Journal of Magnetism and Magnetic Materials, 234, p. 535-544, 2001

[5] Kliava, J. and R. Berger, *Size and Shape Distribution of Magnetic Nanoparticles in Disordered Systems: Computer Simulations of Superparamagnetic Resonance Spectra*. Journal of Magnetism and Magnetic Materials, 205, p. 328-342, 1999

[6] Sharma, V.K. and F. Waldner, *Superparamagnetic and Ferrimagnetic Resonance of Ultrafine Fe_3O_4 particles in ferrofluids*. Journal of Applied Physics, 48, p. 4298-4302, 1977

[7] Usselman, R.J., et al., *Electron Paramagnetic Resonance of Iron Oxide Nanoparticles Mineralized in Protein Cages*. Journal of Applied Physics, 97, p. 10M523 Part 3, 2005

[8] Caruntu, D., et al., *Synthesis of Variable-Sized Nanocrystals of Fe_3O_4 with High Surface Reactivity*. Chemistry Materials, 16, p. 5527-5534, 2004

[9] Koksharov, Y.A., et al., *Electron Paramagnetic Resonance of Ferrite Nanoparticles*. Journal of Applied Physics, 89, p. 2293-2298, 2001

[10] Jones, J.P.E., B.R. Angel, and P.L. Hall, *Electron Spin Resonance Studies of Doped Synthetic Kaolinite. II.* Clay Minerals, 10, p. 257-270, 1974

[11] Berger, R., et al., *Superparamagnetic Resonance of Annealed Iron-containing Borate Glass*. Journal of Physics: Condensed Matter, 10, p. 8559-8572, 1998

[12] Koseoglu, Y., et al., *EPR Studies of Na-oleate coated Fe_3O_4 nanoparticles.* Physica Status Solidi C, 1, p. 3511-3514, 2004

[13] Koseoglu, Y. and B. Aktas, *ESR Studies on Superparamagnetic Fe_3O_4 nanoparticles*. Physica Status Solidi C, 1, p. 3516-3520, 2004

[14] Huang, S.-H., M.-H. Liao, and D.-H. Chen, *Direct Binding and Characterization of Lipase onto Magnetic Nanoparticles*. Biotechnology Progress, 19, p. 1095-1100, 2003

[15] Bickford, L.R., *Ferromagnetic Resonance Absorption Magnetite*. Physics Review, 78, p. 449, 1950

[16] Angel, B.R. and W.E.J. Vincent, *Electron Spin Resonance Studies of Iron Oxides Associated with the Surface of Kaolins*. Clays and Clay Minerals, 26, p. 263-272, 1978